

## Correction The combined hypnotic medicines' synergistic effects on mice's sleep

Dr.M.Kishore Babu, M. Indira, M.Sravya, Reeni Diana

1. Professor , Department of pharmaceutics , QIS College of pharmacy , Ongole , A.P

2. Assistant Professor , Department of Pharmaceutics , QIS College of pharmacy , Ongole , A.P

3. Associate Professor , Department of Pharm D , QIS College of pharmacy , Ongole , A.P

4. Assistant Professor , Department of Pharmaceutics , QIS College of pharmacy , Ongole , A.P

### ABSTRACT:

Our goal in doing this study was to find out how dexmedetomidine (DMED) and eszopiclone (ESZ) worked together to influence mice's ability to sleep.

Researchers used the loss of righting reflex (LORR) as a sleep indicator to study the effects of DMED and ESZ alone and in combination on mice's sleep status. They also recorded sleep-related parameters and used isobolographic analysis to determine how the two drugs interacted with each other. In order to delve deeper into the effects of DMED and ESZ on sleep structure, neurotransmitter levels, and the regulation of c-Fos protein expression in the ventrolateral preoptic area (VLPO) and the tuberomammillary nucleus (TMN), researchers utilized a combination of electroencephalogram/ electromyogram

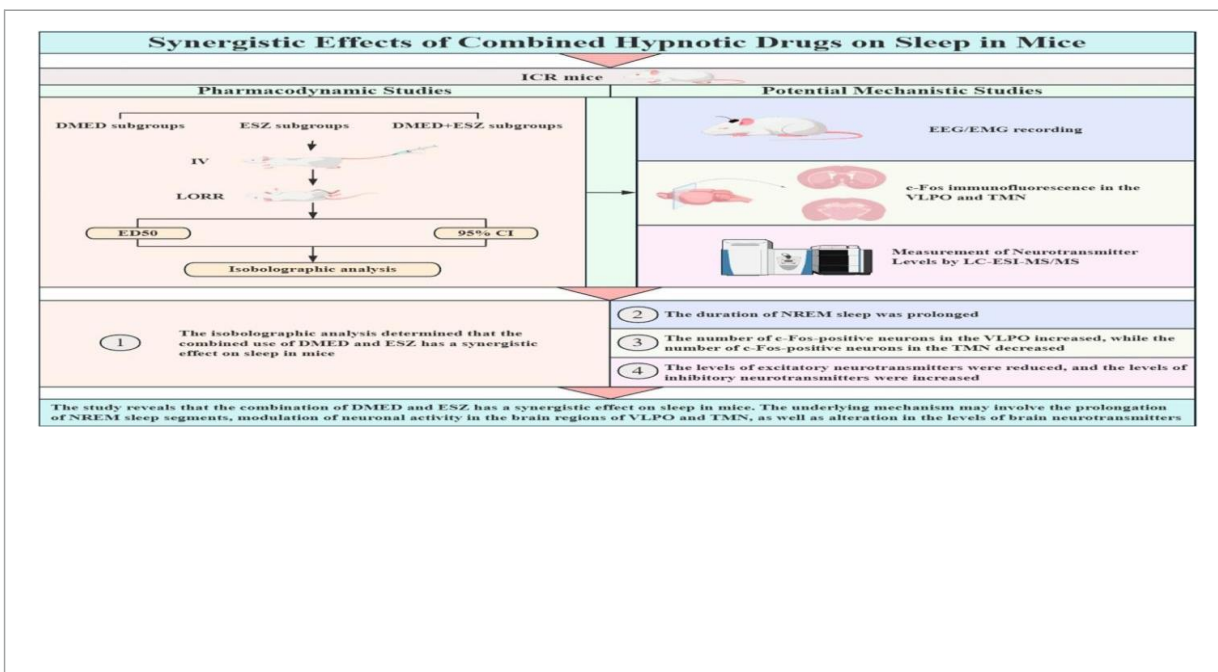
(EEG/EMG) sleep phase analysis, c-Fos immunofluorescence, and brain measurements of neurotransmitter content.

Results: Mice's sleep was improved by a synergistic impact of DMED and ESZ, as shown by isobolographic study. There was a significant increase in the amount of time spent in non-rapid eye movement (NREM) sleep, a reduction in the amount of time spent in TMN sleep, an increase in inhibitory neurotransmitter levels and a decrease in excitatory neurotransmitter levels, and an overall lengthening of NREM sleep.

This research concludes that DMED and ESZ have a synergistic impact on sleep in mice. Possible underlying mechanisms include changes to neurotransmitter levels, regulation of neural activity in the VLPO and TMN brain regions, and an extension of non-REM sleep.

### KEYWORDS

sleep, hypnotics, dexmedetomidine, eszopiclone, combination, synergistic effects



## 1 Introduction

In the biological realm, sleep is a systemic physiological phenomena (Tononi et al., 2024) that plays an essential role in regulating alertness, cognition, learning, and memory while also reducing the breakdown of bodily energy and promoting the clearance of metabolic waste from the brain. According to Baranwal et al. (2023), it also plays a significant role in controlling the body's immune system and the release of physiological hormones. The two main stages of a typical night's sleep—rapid eye movement (REM) sleep and non-rapid eye movement (NREM) sleep—are characterized by differing electroencephalogram (EEG) patterns and behavioral traits. According to Sun et al. (2020), rapid eye movement (REM) sleep is linked to dreaming and cognitive processing, but non-REM sleep is essential for physical recovery, energy storage, and memory consolidation. The brain's neurotransmitter systems control the sleep-wake cycle. Monoaminergic neurons in the anterior brainstem and caudal hypothalamus govern wakefulness via wake-promoting pathways that project directly to the cerebral cortex, hypothalamus, and thalamus. Some examples of monoaminergic neurons are those located in the locus coeruleus (LC) region, which are norepinephrineergic neurons (Bajwa and Kulshrestha, 2013), the dorsal raphe nucleus (DRN), which are dopaminergic neurons (Montero et al., 2021), and the tuberomammillary nucleus (TMN), which are histaminergic neurons (Scammell et al., 2019). The firing frequency of these central neurons is greatest during wakefulness and decreases during non-REM sleep; they produce alertness by stimulating cortical activation and increasing muscular tone simultaneously. Furthermore, the ascending arousal system relies on cholinergic neurons in the laterodorsal tegmental nucleus (LDT) and pedunculopontine nucleus (PPT) (Jones, 2020), whereas the thalamocortical circuit's wakefulness is driven by glutamatergic neurons that mediate amino acid neurotransmission. The ventrolateral preoptic nucleus (VLPO) of the anterior hypothalamus contains gamma-aminobutyric acidergic (GABAergic) neurons that, during non-REM sleep, route their projections to the histaminergic TMN, therefore inhibiting alertness and arousal. On the other hand, sleep problems have become more common as a result of societal advancements including faster living speeds and increased stress levels. Difficulty getting to sleep, staying asleep, waking up often, or waking up early in the morning are common symptoms of these diseases (Hughes et al., 2021). As a consequence, people with these illnesses have trouble functioning throughout the day and their daily life and work are greatly affected. Cognitive behavioral therapy (CBT) is now the gold standard for treating insomnia issues; nevertheless, there are some drawbacks to this approach, such as the length of time it takes to see results.

sedative-hypnotic medications are still the go-to for treating insomnia because of their long half-life and gradual therapeutic start. Despite this, there is a clear pattern to the drug regimens for sleep disorders, and it is marked by ineffectiveness and a plethora of adverse effects. Addiction and cognitive impairment may result from long-term use because it interferes with the brain's reward system (Crowe and Stranks, 2018; He et al., 2019). It has the potential to disrupt neurotransmitter function, which in turn impacts mood regulation (Ciucă Anghel et al., 2023). Zheng et al. (2023) and He et al. (2019) found that it also greatly raises the probability of neurological illnesses. As a result, research into medication combinations for sleep regulation is crucial for reducing the risks associated with high dosages of individual medications. Dexmedetomidine (DMED) is a pharmaceutical agent that acts on  $\alpha$ 2-adrenergic receptors ( $\alpha$ 2-AR) in both the central nervous system and the periphery, namely in the Chima region.

In 2022 (et al.) A few of its benefits include calming the nervous system, reducing inflammation, protecting internal organs, reducing delirium, hypnosis, analgesia, and antisympathetic effects. More and more people are turning to DMED as a solution to their persistent insomnia problems (Ramaswamy et al., 2021). Most people think that DMED makes you sleep by lowering norepinephrine (NE) release via a Gi-coupled mechanism by

activating presynaptic  $\alpha$ 2 receptors on norepinephrine (NE) neurons in the LC (Fan et al., 2023). According to Zhang et al. (2015), DMED is known to activate GABAergic neurons in the lateral preoptic region (LPO), which in turn induces sleep. Research conducted by Wu et al. (2016), Ren et al. (2018), Bao et al. (2021), and Dong et al. (2022) has shown that DMED induces sleep that is comparable to physiologic sleep, without respiratory depression and with enhanced sleep depth. While DMED does have a sedative effect, it is very easy to awaken patients. This unique property of DMED makes it widely used in clinical anesthesia and ICU sedation, although the exact neural mechanism that causes rapid arousability during this process is still unclear. It may involve ventral tegmental area (VTA) dopaminergic neurons (Qiu et al., 2020; Wang et al., 2023; Duan et al., 2024). Furthermore, NREM sleep duration, depth, and quality may all be improved by DMED, according to many research (Feng et al., 2018; Fan et al., 2023). Even yet, DMED isn't without its flaws. Its potential to cause cardiovascular side effects like hypertension, bradycardia, and hypotension due to postsynaptic  $\alpha$ 2-AR activation, along with dose-dependence, tolerance, and withdrawal reactions with long-term use, and higher economic costs, all serve to restrict its use in clinical practice to a certain degree (Weerink et al., 2017). The pyrrolidine derivative of the cyclopyrrolone family, eszopiclone (ESZ) is a GABA receptor agonist that can selectively bind to GABA-A receptors coupled to benzodiazepine receptors. This enhances the inhibitory effect of GABA on neurons and produces sedative, hypnotic, and anxiolytic effects. Eszopiclone is considered a third-generation novel non-benzodiazepine drug (NBZD). Research has also shown that ESZ may promote sleep by inhibiting hypocretin (HCRT) neurons in the lateral hypothalamus (LH), which in turn suppresses the basal forebrain and dopaminergic neurons (DRN). A shorter NREM latency is a hallmark of the sleep that ESZ usually causes.

prolonged NREM sleep duration, and unchanged REM sleep duration (Gerashchenko et al., 2017). It facilitates NREM sleep by enhancing GABAergic transmission in the thalamic reticular nucleus, thereby inducing sleep spindle generation (Wamsley et al., 2013; Dimitrios et al., 2020). ESZ has the advantages of rapid onset of action, short half-life, and few side effects, especially in improving sleep maintenance disorders. Therefore, ESZ is commonly used in the treatment of insomnia and can effectively improve sleep onset and maintenance in patients. Despite the significant advantages of ESZ in the treatment of insomnia, there are some limitations and application drawbacks. It may cause common adverse effects, such as dry mouth, dizziness, fatigue, abnormal taste, and daytime sleepiness (Liang et al., 2019), and long-term use may produce drug dependence and withdrawal reactions. In addition, the tolerability and higher economic cost issues of ESZ have limited its use in clinical settings.

Although DMED and ESZ each have well-defined roles and

advantages in regulating sleep, studies of their combined use have not been reported. Since DMED mainly acts in regions such as the brainstem and hypothalamus, it regulates the noradrenergic system by agonizing  $\alpha$ 2-AR, which in turn inhibits sympathetic activity to induce sleep (Nelson et al., 2003), whereas ESZ mainly acts in regions such as the cerebral cortex, the limbic system, and the thalamus, and promotes sleep by augmenting GABAergic inhibitory neurotransmission, and decreasing the excitability of the cortex and the limbic system (Hanson et al., 2008). The two are complementary in their sites of action and neurotransmitter regulatory pathways, and their combined application may further enhance sleep depth and improve sleep quality. Therefore, the combination is expected to enhance the therapeutic effect while reducing the dose of a single drug, decrease the

occurrence of side effects, and optimize the economic cost of treatment.

For this reason, the present study focused on the combination of DMED and ESZ as an entry point, integrating isobolographic analysis, electroencephalogram/electromyogram (EEG/EMG) sleep monitoring, c-Fos immunofluorescence staining, and liquid chromatography-electrospray ionization-tandem mass spectrometry (LC-ESI-MS/MS) to investigate the interaction between these two drugs on sleep in mice and their potential mechanisms of action. Our results demonstrate that the combination of DMED and ESZ exhibits a synergistic effect on sleep in mice. The underlying mechanism may involve prolonging NREM sleep, modulating neuronal activity in the VLPO and TMN brain regions, and altering brain neurotransmitter levels. These findings provide a robust theoretical basis for clinical combination therapy to improve sleep quality.

## 2 Materials and methods

### 2.1 Experimental animals

Healthy male ICR mice, SPF grade, 6–8 weeks old, weighing 18–20 g, were purchased from Beijing HFK Bioscience Co., Ltd. (Beijing, China). The animals were housed in groups of 4 per cage under controlled conditions: temperature  $22^{\circ}\text{C} \pm 2^{\circ}\text{C}$ , humidity  $50\% \pm 10\%$ , and a 12 h/12 h light-dark cycle (light on/off time: 08:00/20:00). Standard feed and water were provided *ad libitum*. The animal welfare and experimental project were approved by the Animal Ethics Committee of State Key Laboratory of NBC Protection for Civilian, and every effort was made in the experiment to reduce the number of animals used and any pain or discomfort they might experience.

### 2.2 Drugs, reagents, and instruments

Dexmedetomidine (315988, Hebei Pinkeyan Biotechnology Co., Ltd., China); Eszopiclone (2410892Z-YT-01, Standard Drug Group Co., Ltd., China); Pentobarbital sodium (63-06-01, Shanghai Chemical Reagent Procurement and Supply Station, China); Triton X-100 (30188928, Sinopharm Group, China); OCT embedding agent (Sakura Finetek, United States); Rabbit anti-c-Fos antibody (ab222699, Abcam, United States); Goat anti-rabbit secondary antibody (A32740, Thermo Fisher Scientific, United States). Dopamine (Z21J10R91113, Shanghai Yuanye Bio-Technology Co., Ltd., China); Norepinephrine (H01M10C81693, Shanghai Yuanye Bio-Technology Co., Ltd., China); 5-Hydroxytryptophan (111656-200401, National Institutes for Food and Drug Control, China); 5-Hydroxyindole-3-Acetic Acid (21A020-I9, SHANGHAI ZZBIO CO., LTD., China);  $\gamma$ -Aminobutyric acid (Z07J10H79273, Shanghai Yuanye Bio-Technology Co., Ltd., China); Acetylcholine (Z08N8H47718, Shanghai Yuanye Bio-Technology Co., Ltd., China); Histamine (X17S9B70455, Shanghai Yuanye Bio-Technology Co., Ltd., China); Glutamic acid (S12A10I85582, Shanghai Yuanye Bio-Technology Co., Ltd., China); HPLC grade-acetonitrile (A998-4, Thermo Fisher Scientific, United States); HPLC grade-methanol (A452-4, Thermo Fisher Scientific, United

States); formic acid (UN 1779, CNW Technologies GmbH, Germany); LCMS grade-purified water (W6-4, Thermo Fisher Scientific, United States).

Leica cryostat (CM 1950, Leica Biosystems, Germany); Confocal microscope (Stellaris5, Leica Biosystems, Germany); Circuit board soldering iron (SBK936B, BAKON Electronic Technology Co., Ltd., China); Miniature cranial drill (RWD Life science Co., Ltd., China); Stereotaxic apparatus (71000-M, RWD Life science Co., Ltd., China); Small animal sleep analysis and detection system (8200- K1, Pinnacle Technologies Co., Ltd., United States); Liquid chromatography-mass spectrometer (QTRAP 6500+, AB SCIEX); Cryo-mill (Wonbio-96E, Shanghai Wanbai Biotechnology Co., Ltd., China); Ultrasonic Cleaner (SBL-10DT, NingBo Scientz Biotechnology Co., Ltd., China); Freezing Centrifuge Concentration Dryer (LNG-T98, Taicang Huamei Biochemical Instrument Factory, China).

### 2.3 Pharmacodynamic study of DMED and ESZ alone

Grouping and administration: ICR mice aged 6–8 weeks were selected for the study and divided into a control group (Control group) and experimental groups (DMED group, ESZ group, and DMED+ESZ group) using the random number table method. Each experimental group was further divided into 5 subgroups according to the different drug doses, and different doses of drugs, respectively, were given by intravenous (IV) injection via the caudal vein with a volume of 0.1 mL/10 g.

Preparation of drugs for IV injection: DMED was dissolved in 100% dimethyl sulfoxide (DMSO) to prepare a 2 mg/mL stock solution, which was aliquoted and stored at  $-20^{\circ}\text{C}$  to preserve stability. Before intravenous injection, the stock solution was further diluted with 0.9% saline to achieve the desired dose. The final DMSO concentration in the injected solution was  $\leq 1\%$  (v/v), ensuring biocompatibility and minimal solvent-related toxicity. ESZ was dissolved in 50 mM sodium acetate buffer (pH  $4.5 \pm 0.1$ ) to prepare a 20 mg/mL stock solution, aliquoted, and stored at  $-20^{\circ}\text{C}$  to maintain stability. The stock solution was diluted with 0.9% sterile saline immediately prior to intravenous administration to achieve desired concentrations.

Determination of administration dose: Mice in each experimental group were subjected to the loss of righting reflex (LORR) experiment. After the administration of the drug, the mice were gently placed in the cage in the supine position, and the mice were turned over once every 1 min; if they remained in the supine position for  $\geq 1$  min, it was determined as LORR; if the mice were restored to the prone position for  $\geq 2$  times in 1 min, it was judged as recovery of the turning-right reflex (Revel et al., 2009). The LORR was used as the criterion to obtain the minimum dose ( $\text{ED}_{100}$ ) with a 100% response rate to DMED and ESZ hypnosis and the maximum dose ( $\text{ED}_0$ ) with a 0% response rate in mice, respectively. Within this dose range, it was divided into 5 dose groups in an equiproportional series, and the common ratio ( $r$ ) of the doses of each group was  $r = \sqrt[5]{-1} \text{ED}_{100}/\text{ED}_0$ , and after obtaining  $r$ , the dose of the next adjacent group was obtained by multiplying  $r$  from the first dose group ( $\text{ED}_0$ ), that is to say, the doses of each group were  $\text{ED}_0, r \cdot \text{ED}_0, r^2 \cdot \text{ED}_0, r^3 \cdot \text{ED}_0, r^4 \cdot \text{ED}_0, r^5 \cdot \text{ED}_0$ .

The sleeping rate, sleep latency, and total sleep time were recorded for each group of mice following drug administration. The  $\text{ED}_{50}$  and its 95% confidence interval (CI) of DMED and ESZ alone were calculated using the Bliss method.

## 2.4 Pharmacodynamic study of DMED and ESZ in combination

After obtaining the respective median effective doses (ED<sub>50</sub>) of DMED and ESZ, fixed-dose combinations were administered based on the ratio of DMED's ED<sub>50</sub> to ESZ's ED<sub>50</sub> (DMED's ED<sub>50</sub>:ESZ's ED<sub>50</sub>). The experimental methodology followed the same procedures as described for individual drug administration. Isobolographic analysis was employed to assess the interaction between the two drugs. The ED<sub>50</sub> of DMED in the combination and its 95% CI were plotted on the x-axis, while the ED<sub>50</sub> of ESZ and its 95% CI were plotted on the y-axis. A line connecting the two ED<sub>50</sub> points was drawn to represent the additive effect line, and the 95% CI lines were connected to establish the 95% CI of the additive line. The ED<sub>50</sub> of the combined treatment was then plotted on the same coordinate axis. If the ED<sub>50</sub> of the combined treatment fell on the additive line or within its 95% CI, the interaction was considered additive. If it fell to the left of the additive line and its 95% CI, the interaction was synergistic. Conversely, if it fell to the right of the additive line and its 95% CI, the interaction was antagonistic.

TABLE 1 EEG power analysis definition rules.

Name	Low frequency	High frequency
Full	0	1,000
Alpha	8	13
Beta	13	30
Gamma	35	44
Delta	0.5	4
Theta	5.5	8.5

TABLE 2 EMG power analysis definition rules.

Name	Low frequency	High frequency
Full	0	1,000
10~50	10	50
50~100	50	100
100~150	100	150
150~200	150	200
50~150	50	150

## 2.5 Burial of EEG/EMG

Mice were anesthetized via intraperitoneal injection of 1% sodium pentobarbital (70 mg/kg body weight). The heads and necks of the mice were shaved and securely positioned in a brain stereotaxic apparatus. EEG and EMG electrodes were surgically implanted into the skull following a previously established protocol (Sharma et al., 2018), small holes were drilled into the skull, and stainless steel screws were inserted as EEG electrodes. The entire device was then anchored to the skull using dental cement. After the cement had fully cured, two insulated silver

electrode wires for EMG recording were inserted bilaterally into the trapezius muscles of the neck. Residual cement around the surgical site was carefully removed, and the incision was closed with sutures. The mice were placed in a lateral recumbent position on a 37°C temperature-controlled heating pad to recover until fully conscious. Experimental recordings were conducted 1-week post-surgery to allow for postoperative recovery.

## 2.6 EEG/EMG data recording and processing

Twenty-four mice exhibiting normal EEG and EMG signal patterns were selected and randomly assigned to four groups ( $n = 6$  per group): Control group, DMED group, ESZ group, and DMED+ESZ group. Each mouse was placed in a sleep-monitoring chamber for continuous sleep-stage data acquisition. EEG and EMG recordings commenced at 08:00 and lasted for 12 h. The 12-h EEG and EMG voltage traces were segmented into 4,320 epochs, with each epoch lasting 10 s. Power thresholds for EEG and EMG were defined for each epoch based on energy values (criteria detailed in Tables 1, 2). The recorded data were exported and processed using Sirenia Acquisition 2.1.5 software to generate voltage-time plots for individual mice. These plots were subsequently analyzed in Sirenia Sleep 2.1.5 software to quantify the duration of distinct sleep-wake states, including wakefulness (Wake), non-rapid eye movement (NREM) sleep, and rapid eye movement (REM) sleep. Additionally, graphical representations of state transitions were generated to visualize temporal changes between these states.

## 2.7 Preparation of brain tissue and frozen section

All experimental mice were deeply anesthetized via intraperitoneal injection of 1% sodium pentobarbital (70 mg/kg body weight) 1.5 h after drug administration. Following anesthesia, a thoracotomy was performed to expose the heart for transcardial perfusion fixation. Perfusion was conducted sequentially: first with 30 mL of phosphate buffered saline (PBS, 0.01 M, pH 7.4) to clear intravascular blood, followed by 30 mL of 4% paraformaldehyde (PFA) solution for fixation. The fresh brain tissues were fixed in 4% PFA solution for 24 h at 4°C and then dehydrated sequentially through a gradient of 10%, 20%, and 30% sucrose solution, with replacement to a higher concentration signified by the tissues sinking to the bottom. Once they had sunk to the bottom in 30% sucrose solution, they were ready for frozen sectioning. For this experiment, OCT (Optimal cutting temperature compound) embedding was used, and continuous coronal sectioning was carried out using a Leica cryostat with a section thickness of 30  $\mu$ m.

## 2.8 c-Fos immunofluorescence

Sections were treated with 3.0% hydrogen peroxide for 25 min and rinsed with phosphate-buffered saline containing 0.1% Tween- 20 (PBST). Sections were then blocked using bovine serum albumin (BSA) containing 0.3% Triton x-100 for 2 h at 4°C. After rinsing, sections were incubated with rabbit-derived primary anti-c-Fos antibody (1:1000 in PBS) overnight at 4°C. After rinsing, sections were placed with goat anti-rabbit

secondary antibody (1:500 in PBS) for 1 h at 37°C, were dropwise added with anti-fade mounting medium (with DAPI), and then sealed with a cap. The stained sections were observed under a confocal microscope at  $\times 20$  and  $\times 40$  magnification. Cells with immunofluorescence intensity exceeding twice the background level were classified as c-Fos positive. Three brain sections containing the target nuclei were counted, and the number of c-Fos positive cells in the VLPO and TMN was quantified using ImageJ software with the Cell Counter plugin.

individual stock solutions. Appropriate volumes of each stock solution were mixed to create a combined standard solution, which was then diluted with water to the desired concentration to prepare the working standard solution. Isotope-labeled standards (Trp-D5 and Glu-13C5) were also accurately weighed and dissolved in methanol to prepare individual stock solutions. These isotope-labeled stock solutions were then mixed and diluted with water to prepare an isotopic internal standard mixture at concentrations of 5,000 ng/mL and 1,000 ng/mL.

Following transcardial perfusion, the whole brain was rapidly dissected for further experiments. The dissected brain tissues were placed into 2 mL EP tubes. Steel beads, 20  $\mu$ L of isotope internal standard (5,000 ng/mL), and 480  $\mu$ L of 80% methanol aqueous solution were added to the tubes. The samples were homogenized using a tissue lyser, incubated at -20°C for 30 min, and then centrifuged at 14,000 g for 15 min at 4°C. A total of 250  $\mu$ L of the supernatant was transferred to a new tube and dried by centrifugal evaporation. The dried residue was resuspended in ultrapure water via vortexing, followed by centrifugation at 14,000  $\times$  g for 5 min. The resulting supernatant was then transferred to a vial for HPLC-MS/MS analysis to obtain the low-concentration test sample. For the high-concentration sample, 5  $\mu$ L of the original supernatant was mixed with 245  $\mu$ L of ultrapure water by vortexing. Subsequently, 50  $\mu$ L of this diluted solution was combined with 50  $\mu$ L of isotope internal standard (1,000 ng/mL). After thorough vortexing and centrifugation at 14,000  $\times$  g for 5 min, the supernatant was transferred to a separate vial, yielding the high-concentration test sample.

## 2.10 Determination of neurotransmitter levels

LC-ESI-MS/MS was used to quantify the target compounds in the samples. Chromatographic conditions: ExionLC AD system, Waters HSS T3 (2.1  $\times$  100 mm, 1.8  $\mu$ m) liquid chromatography column, column temperature 35°C, injection volume 1  $\mu$ L. Mobile phase A was 0.1% formic acid in water, and mobile phase B was 0.1% formic acid in acetonitrile. The chromatographic gradients are shown in Table 3. Mass spectrometry conditions: AB SCIEX QTRAP 6500+ with positive/negative mode detection, Curtain Gas (CUR) of 35 psi, Collision Gas (CAD) of Medium, IonSpray Voltage (IS) of +5,500/-4,500 V, Temperature (TEM) of 550°C, Ion

## 2.9 Neurotransmitter standard solution preparation and sample processing

Accurate amounts of standard compounds, including norepinephrine (NE), dopamine (DA), 5-hydroxytryptamine (5-HT), 5-hydroxyindoleacetic acid (5-HIAA),  $\gamma$ -aminobutyric acid (GABA), histamine (His), acetylcholine (Ach), and L-glutamic acid (Glu), were weighed and dissolved in methanol or water to prepare

Source Gas1 (GS1) is 55 psi, and Ion Source Gas2 (GS2) is 55 psi. Default parameters were used in the AB Sciex quantitative software OS for the automatic identification and integration of each ionic fragment with the aid of manual checking. A linear regression standard curve was plotted using the ratio of the mass spectral peak area of the analyte to the peak area of the internal standard as the vertical coordinate and the concentration as the horizontal coordinate. To calculate the sample concentration: The ratio of the mass spectral peak area of the sample analyte to the peak area of the internal standard is substituted into the linear equation to calculate the concentration result.

TABLE 3 Chromatographic gradients.

Time (min)	Flow rate (mL/min)	A%	B%
0.00	0.30	100.0	0.0
1.00	0.30	100.0	0.0
3.00	0.30	95.0	5.0
5.00	0.30	90.0	10.0
6.00	0.30	85.0	15.0
7.00	0.30	85.0	15.0
10.00	0.30	40.0	60.0
11.00	0.30	0.0	100.0
12.00	0.30	0.0	100.0
12.01	0.30	100.0	0.0
13.00	0.30	100.0	0.0
15.00	0.30	100.0	0.0

## 2.11 Statistics and analysis of data

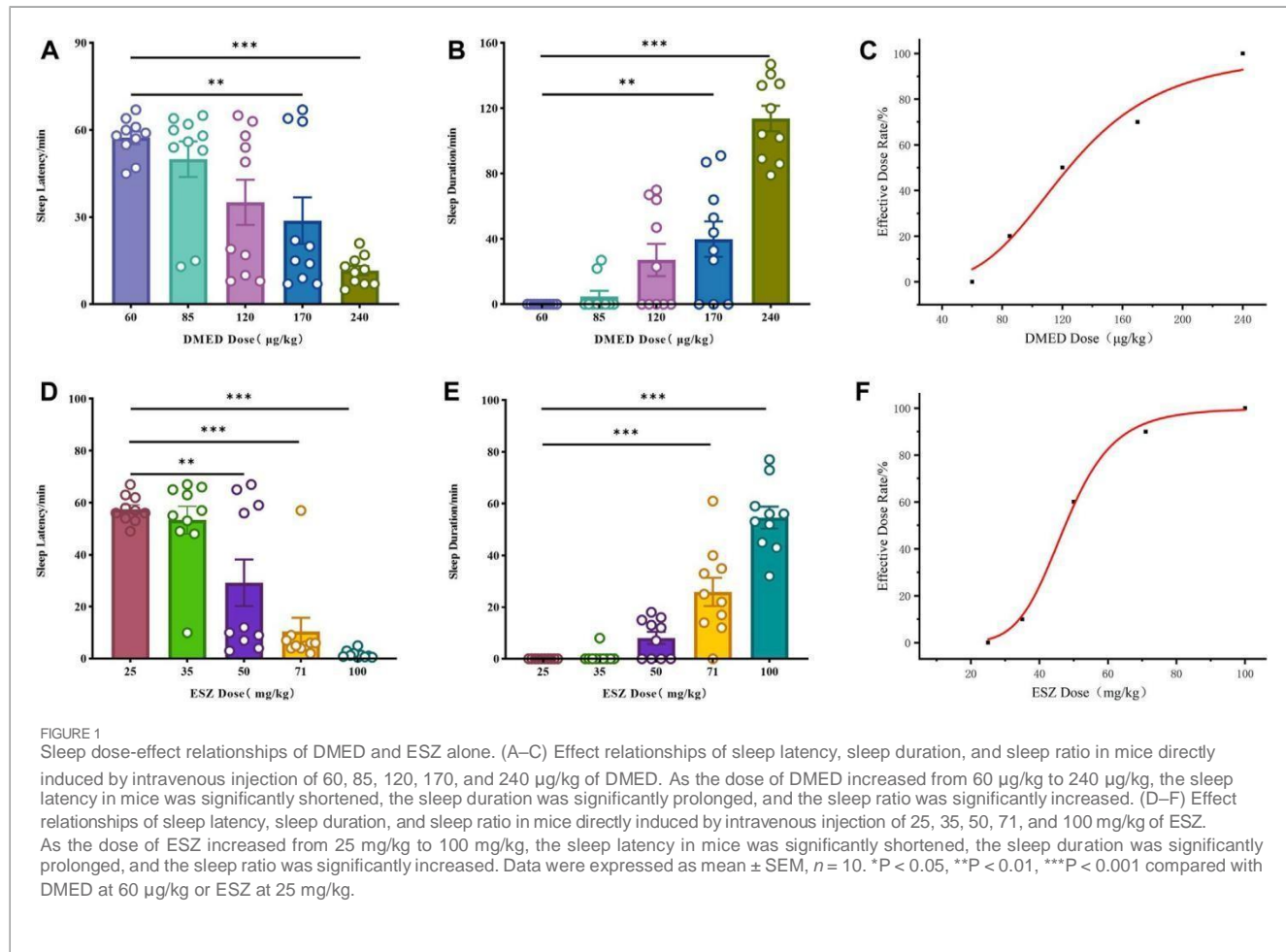
The experimental data were presented as Mean  $\pm$  SEM. Statistical analyses were performed using GraphPad Prism version 9.1.0 for Windows (GraphPad Software, La Jolla, CA, United States). One-way analysis of variance (one-way ANOVA) followed by Bonferroni's *post hoc* test for multiple comparisons was used to analyze the data. The significance threshold was set at  $p < 0.05$ .

## 3 Results

### 3.1 Dose-effect relationship between DMED and ESZ alone on sleep in mice

The initial results revealed that the minimum doses (ED<sub>100</sub>)

of DMED and ESZ required to achieve a 100% hypnotic response rate in mice were 240  $\mu\text{g}/\text{kg}$  and 100  $\text{mg}/\text{kg}$ , respectively, while the maximum doses ( $\text{ED}_{100}$ ) resulting in a 0% response rate were 60  $\mu\text{g}/\text{kg}$  and 25  $\text{mg}/\text{kg}$ , respectively. Accordingly, the five subgroup doses for the DMED group were set at 60  $\mu\text{g}/\text{kg}$ , 85  $\mu\text{g}/\text{kg}$ , 120  $\mu\text{g}/\text{kg}$ , 170  $\mu\text{g}/\text{kg}$ , and 240  $\mu\text{g}/\text{kg}$ , and for the ESZ group, they were 25  $\text{mg}/\text{kg}$ , 35  $\text{mg}/\text{kg}$ , 50  $\text{mg}/\text{kg}$ , 71  $\text{mg}/\text{kg}$ , and 100  $\text{mg}/\text{kg}$ . As the dose of DMED increased from 60  $\mu\text{g}/\text{kg}$  to 240  $\mu\text{g}/\text{kg}$ , the sleep latency in mice was significantly shortened (Figure 1A), the sleep duration was significantly prolonged (Figure 1B), and the sleep ratio was significantly increased (Figure 1C). The hypnotic  $\text{ED}_{50}$  for DMED was determined to be 124  $\mu\text{g}/\text{kg}$ , with a 95% confidence interval ranging from 103.4  $\mu\text{g}/\text{kg}$  to 150.1  $\mu\text{g}/\text{kg}$ . Similarly, as the dose of ESZ increased from 25  $\text{mg}/\text{kg}$  to 100  $\text{mg}/\text{kg}$ , the sleep latency was significantly reduced (Figure 1D), the sleep duration was significantly extended (Figure 1E), and the sleep ratio was significantly elevated (Figure 1F). The hypnotic  $\text{ED}_{50}$  for ESZ was calculated to be 48  $\text{mg}/\text{kg}$ , with a 95% CI of 41.2  $\text{mg}/\text{kg}$  to 56.6  $\text{mg}/\text{kg}$ .



### 3.2 Interaction between DMED and ESZ combination on sleep in mice

DMED and ESZ were co-administered at a fixed dose ratio based on their respective half-effective doses (124:48000, approximately 1:387.1). In previous experiments, the minimum doses ( $\text{ED}_{100}$ ) required to achieve a 100% hypnotic response rate in mice were determined to be 48.0  $\mu\text{g}/\text{kg}$  for DMED and 18.6  $\text{mg}/\text{kg}$  for ESZ, while the maximum doses ( $\text{ED}_0$ ) resulting in a 0% response rate were 3.0  $\mu\text{g}/\text{kg}$  for DMED and 1.2  $\text{mg}/\text{kg}$  for ESZ. Accordingly, the five subgroup doses for the combined DMED+ESZ group were set as follows: 3.0  $\mu\text{g}/\text{kg}$  + 1.2  $\text{mg}/\text{kg}$ , 6.0  $\mu\text{g}/\text{kg}$  + 2.3  $\text{mg}/\text{kg}$ , 12.0  $\mu\text{g}/\text{kg}$  + 4.6  $\text{mg}/\text{kg}$ , 24.0  $\mu\text{g}/\text{kg}$  + 9.3  $\text{mg}/\text{kg}$ , and 48.0  $\mu\text{g}/\text{kg}$  + 18.6  $\text{mg}/\text{kg}$ . As the doses increased, the sleep latency gradually decreased (Figure 2A), and the sleep duration progressively prolonged (Figure 2B). The median hypnotic dose ( $\text{ED}_{50}$ ) was achieved at a DMED dose of 11.0  $\mu\text{g}/\text{kg}$ , with a 95% CI ranging from 8.5  $\mu\text{g}/\text{kg}$  to 13.8  $\mu\text{g}/\text{kg}$ , and an ESZ dose of 4.4  $\text{mg}/\text{kg}$ , with a 95% CI ranging from 3.1  $\text{mg}/\text{kg}$  to 6.2  $\text{mg}/\text{kg}$ . In the isobologram (Figure 2C), the coordinates  $a$  and  $c$  on the axes represent the  $\text{ED}_{50}$  values of ESZ and DMED when administered alone, respectively, with dashed lines indicating their 95% CIs. The line connecting points  $a$  and  $c$  represents the additive line. Point  $b$  represents the  $\text{ED}_{50}$  of the combined administration of the two drugs. The nature of the drug interaction is determined by the location of the combined  $\text{ED}_{50}$  relative to the additive line: if it falls to the left of the additive line, the drugs exhibit a

synergistic effect; if it falls to the right, they exhibit an antagonistic effect; and if it lies on the additive line, the effect is additive. Since point b falls to the left of the 95% CI of the additive line, it can be concluded that the combined administration of DMED and ESZ exerts a synergistic effect on sleep induction in mice.

### 3.3 Effects of the combination of DMED and ESZ on the temporal phase of sleep

Based on the aforementioned pharmacodynamic experiments, we selected the combined dose achieving ED100 for further pharmacological studies to investigate the synergistic effects on sleep. Specifically, the DMED group received DMED at 48.0  $\mu$ g/kg, the ESZ group received ESZ at 18.6 mg/kg, the DMED+ESZ group received both DMED at 48.0  $\mu$ g/kg and ESZ at 18.6 mg/kg, and the Control group received an equivalent volume of saline. Due to the inverse circadian rhythm of rodents compared to humans, mice are primarily in a sleep or resting state during the daytime. To explore the regulatory effects of DMED and ESZ on daytime sleep-wake cycles under natural circadian conditions, this experiment was conducted during the light phase, corresponding to the resting period of mice. Figure 3A illustrates the characteristic EEG and EMG patterns of Wake, NREM, and REM phases. The Wake phase is characterized by low-amplitude, high-frequency EEG waves accompanied by significant EMG activity. The NREM phase is marked by high-amplitude, low-frequency EEG waves with minimal EMG activity. The REM phase exhibits low-amplitude, high-frequency EEG waves, and similarly, EMG activity is nearly absent. Compared with the Control group, the DMED, ESZ, and DMED+ESZ groups all showed significantly reduced wakefulness

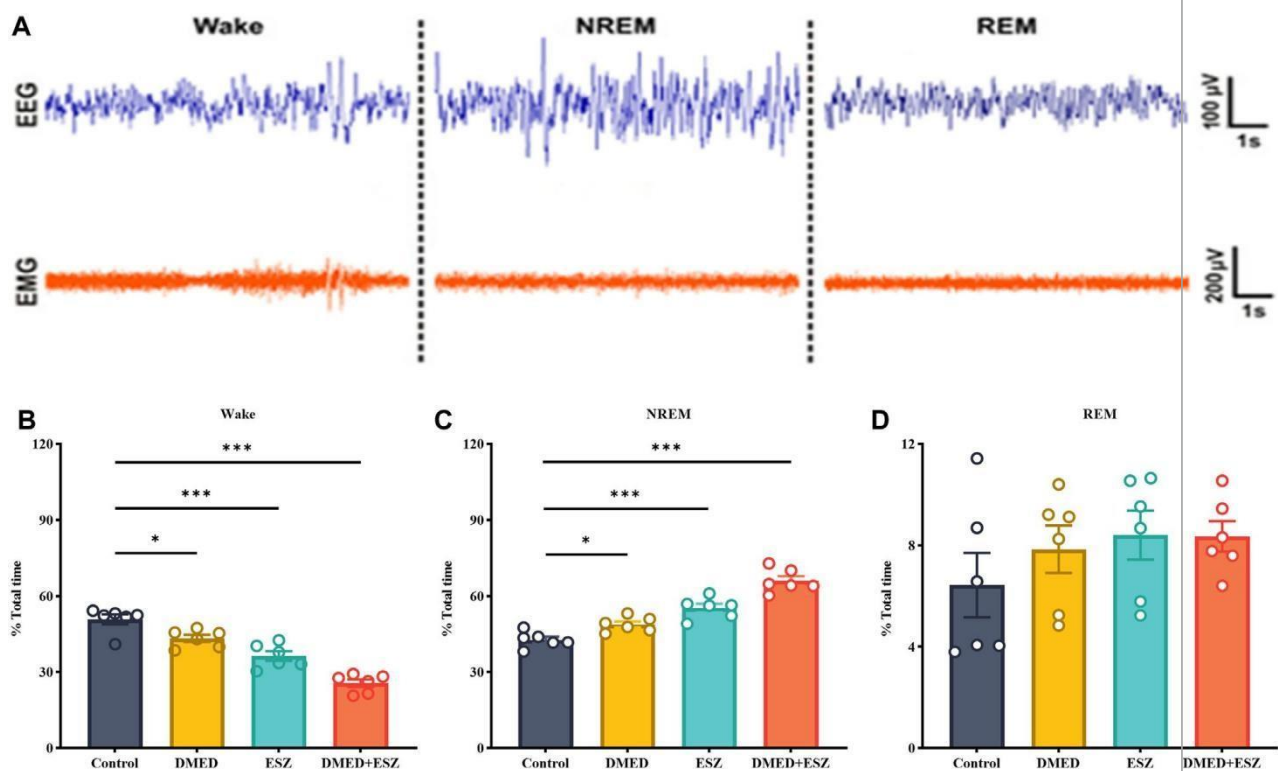


**FIGURE 3**  
Effect of DMED and ESZ combination on sleep phases. (A) Characteristic EEG and EMG patterns of Wake, NREM, and REM phases. The Wake phase is characterized by low-amplitude, high-frequency EEG waves accompanied by significant EMG activity. The NREM phase is marked by high-amplitude, low-frequency EEG waves with minimal EMG activity. The REM phase exhibits low-amplitude, high-frequency EEG waves, and similarly, EMG activity is nearly absent. (B–D) Proportions of Wake, NREM, and REM sleep phases. Compared with control group, the wakefulness duration was significantly shortened and the NREM duration was significantly prolonged in the DMED group, ESZ group, and DMED+ESZ group, while there was no significant change in REM duration. Notably, the NREM duration in the DMED+ESZ group was significantly longer than that in the monotherapy groups. Data were expressed as mean  $\pm$  SEM,  $n = 6$ , \* $P < 0.05$ , \*\* $P < 0.01$ , \*\*\* $P < 0.001$  compared with control.

(Figure 3B; DMED vs. Control,  $p < 0.05$ ; ESZ vs. Control,  $p < 0.001$ ; DMED+ESZ vs. Control,  $p < 0.001$ ) and significantly prolonged

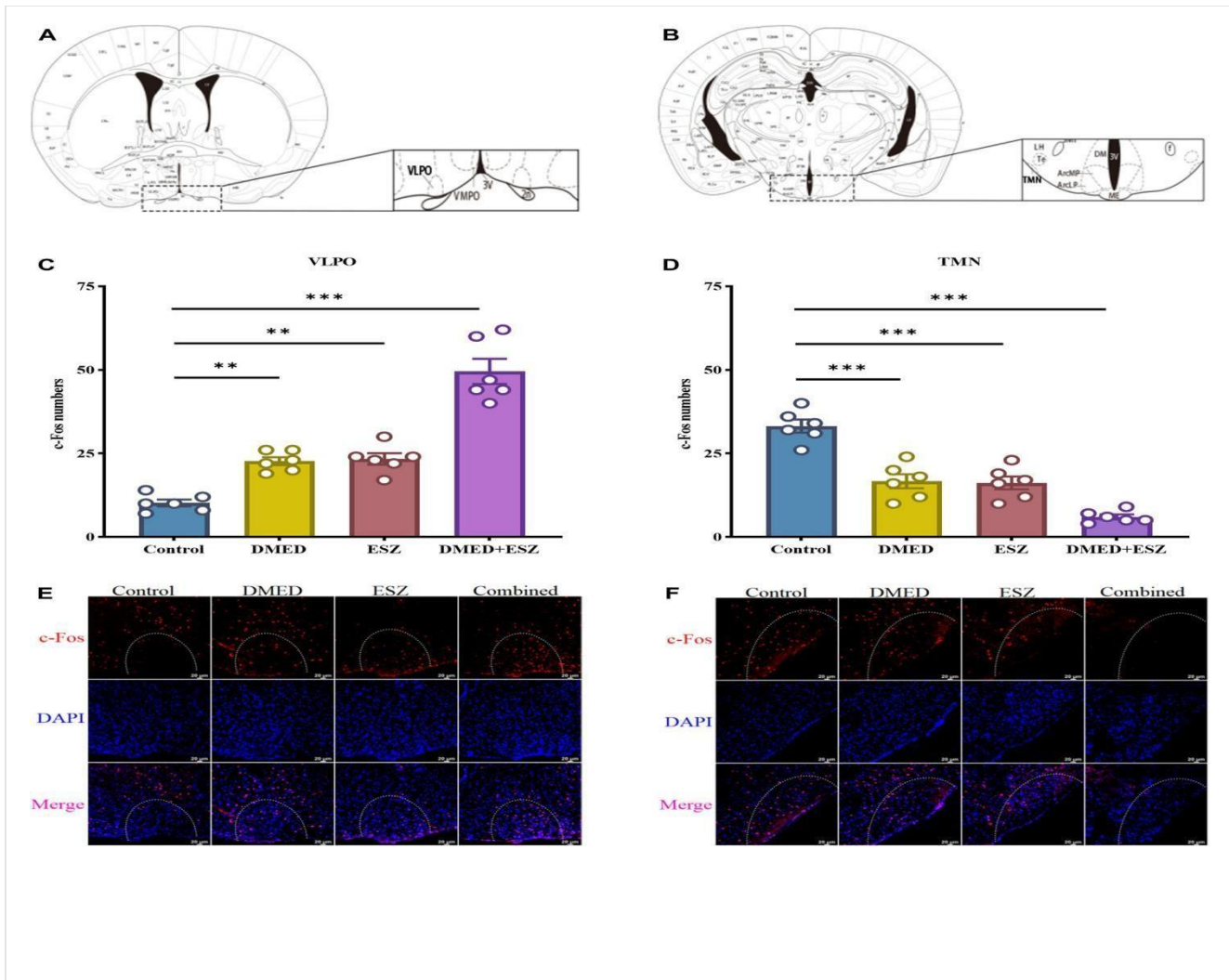


FIGURE 4

Expression of c-Fos neurons in hypothalamic VLPO and TMN after different treatments. (A,B) VLPO brain region, TMN brain region, (C,D) c-Fos positive neuron expression in VLPO, c-Fos positive neuron expression in TMN, (E,F) IF images of c-Fos positive neurons in VLPO and TMN. Compared with the control group, the number of c-Fos positive neurons in the VLPO increased in the DMED group, ESZ group, and DMED+ESZ group. Notably, the DMED+ESZ combination group showed twice as many c-Fos positive neurons in the VLPO as the monotherapy groups. Contrary to the VLPO results, the number of c-Fos-positive neurons in the TMN decreased in the DMED group, ESZ group, and DMED+ESZ group compared with the control group after drug administration. The reduction in the number of positive neurons in the combination group was 1.6-fold that of the monotherapy groups. Data were expressed as mean  $\pm$  SEM,  $n = 3$ , \*\* $P < 0.01$ , \*\*\* $P < 0.001$  compared with control.

NREM duration (Figure 3C; DMED vs. Control,  $p < 0.05$ ; ESZ vs. Control,  $p < 0.001$ ; DMED+ESZ vs. Control,  $p < 0.001$ ). Notably, the NREM duration in the DMED+ESZ group was significantly longer than that in the monotherapy groups (DMED+ESZ vs. DMED,  $p < 0.001$ ; DMED+ESZ vs. ESZ,  $p < 0.001$ ). However, no significant changes were observed in REM duration (Figure 3D; DMED+ESZ vs. Control,  $P > 0.05$ ). These results are consistent with the isobolographic analysis indicating a synergistic effect of DMED

and ESZ on sleep in mice. Furthermore, they suggest that the combination of DMED and ESZ may exert its synergistic effects by prolonging the NREM phase of the sleep architecture.

### 3.4 Regulation of c-fos positive neuronal expression in VLPO and TMN brain regions by the combination of DMED and ESZ

The results are shown in Figures 4A,C,E. The control group exhibited the lowest number of c-Fos positive neurons due to the subthreshold nature of low-frequency tonic firing activity in VLPO neurons during natural sleep, which was insufficient to induce c-Fos expression. In contrast, the DMED, ESZ, and DMED + ESZ groups showed an increase in the number of c-Fos positive neurons in the VLPO. Notably, the number of c-Fos positive neurons in the VLPO of the DMED+ESZ group was twice that of the monotherapy groups ( $P < 0.001$ ). This finding is consistent with the observed sleep state in mice following drug administration. In contrast, the number of c-Fos

positive neurons in the TMN significantly decreased after drug administration (Figures 4B,D,F). Compared to the control group, the number of c-Fos positive neurons in the TMN decreased by 50% ( $P < 0.001$ ), 51% ( $P < 0.001$ ), and 82% ( $P < 0.001$ ) in the DMED, ESZ, and DMED+ESZ groups, respectively. Importantly, the reduction in c-Fos positive neurons in the combined treatment group was 1.6 times greater than that in the monotherapy groups ( $P < 0.01$ ).

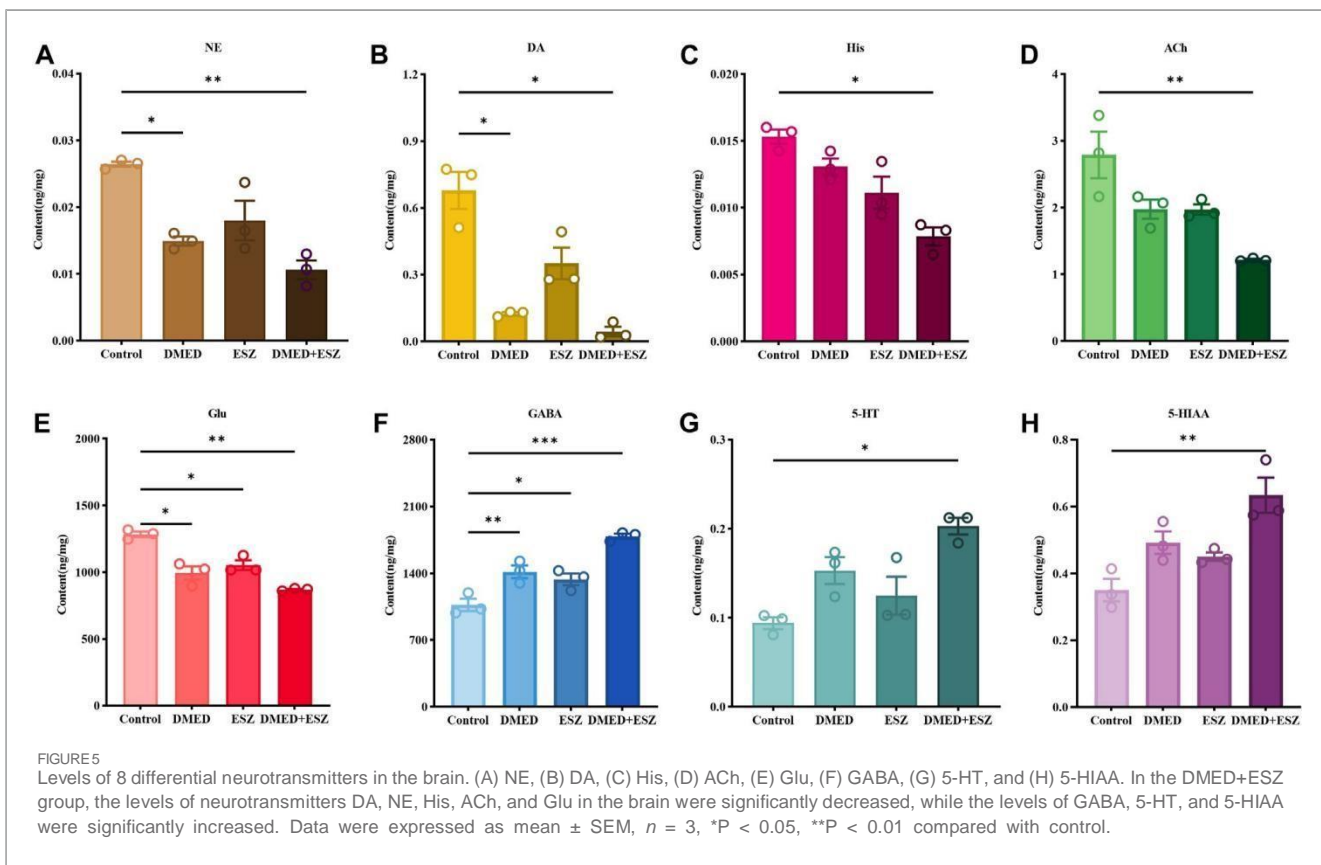
### 3.5 Modulation of neurotransmitter levels in the brain by the combination of DMED and ESZ

The eight neurotransmitters in the brain, NE, DA, His, Ach, Glu, GABA, 5-HT and 5-HIAA were detected and analyzed in this experiment. The experimental results showed that the total ion chromatograms exhibited high resolution and well-defined peaks for all indicators. A linear regression standard curve was plotted with the ratio of the chromatographic peak area of the target standard solution to the internal standard peak area as the y-axis and the concentration as the x-axis. The linearity ( $R^2$ ) for all indicators exceeded 0.99, indicating excellent linearity. Quantitative calculations were performed based on the standard curves. As shown in Figure 5, compared to the control group, intravenous administration of DMED and ESZ individually resulted in a decreasing trend in the levels of NE, DA, Ach, Glu, and His in brain tissue, while the levels of 5-HT, 5-HIAA, and GABA showed an increasing trend. After combined administration of DMED and ESZ, the levels of NE ( $P < 0.05$ ), DA ( $P < 0.01$ ), His ( $P < 0.05$ ), Ach ( $P < 0.01$ ), and Glu ( $P < 0.01$ ) were significantly reduced, whereas the levels of GABA ( $P < 0.001$ ), 5-HT ( $P < 0.05$ ), and 5-HIAA ( $P < 0.05$ ), were significantly increased. These results suggest that the combined use of DMED and ESZ may exert a synergistic regulatory effect on sleep by altering neurotransmitter levels, specifically by reducing excitatory neurotransmitter levels (including NE, DA, His, ACh and Glu) and increasing inhibitory neurotransmitter levels (including GABA, 5-HT and 5-HIAA), thereby modulating neural activity.

## 4 Discussion

The dose-response relationships for sleep induction by DMED and ESZ administered individually were determined using the LORR experiment. The results demonstrated that both DMED and ESZ significantly shortened sleep latency (Figures 1A,D), prolonged the total sleep time in mice (Figures 1B,E), and the sleep rate increased markedly with higher doses (Figures 1C,F). The  $ED_{50}$  for DMED was 124  $\mu$ g/kg, and for ESZ, it was 48 mg/kg. In the combination drug experiment, the  $ED_{50}$  for sleep induction was achieved at a DMED dose of 11.0  $\mu$ g/kg and an ESZ dose of 4.4 mg/kg. Compared to individual administration, the doses required to achieve the same effect in the combined treatment were reduced by more than 11-fold, indicating a significantly greater effect than simple additive interactions. To further clarify the interaction between DMED and ESZ in combination, we employed the isobolographic analysis, a classical method for evaluating drug interactions. This approach offers the advantage of providing a visual and quantitative assessment of the interaction between two or more drugs, making it particularly valuable in pharmacological research (Tallarida, 2011; Foucquier and Guedj, 2015). The isobolographic analysis revealed that the  $ED_{50}$  of the combined treatment fell to the left of the additive line, indicating a synergistic effect between the two drugs in inducing sleep (Figure 2C). To the best of our knowledge, this is the first preclinical study to demonstrate synergistic sleep regulation by combined DMED and ESZ administration in mouse models. Although this specific drug combination has not yet been clinically implemented for human sleep disorders, our findings provide a mechanistic foundation for translational research. From a clinical perspective, such combination therapy may substantially reduce required doses of individual agents, thereby minimizing side effects associated with high-dose monotherapy. Furthermore, for patients with sleep disorders refractory to monotherapy, the DMED-ESZ combination constitutes a novel therapeutic strategy that may enhance clinical efficacy and improve sleep quality.

The sleep-wake state is mainly divided into three states: NREM, REM, and Wake, each characterized by distinct electroencephalogram (EEG) features. During NREM sleep, EMG signals nearly disappear, the overall EEG frequency slows down, the amplitude increases, and Delta waves become significantly enhanced. During REM sleep, EMG signals also nearly disappear, but the overall EEG frequency increases, the amplitude decreases, and Theta waves become notably enhanced. In contrast, during the Wake phase, EMG signals are significantly enhanced, the overall EEG frequency increases, and the amplitude decreases (Scammell et al., 2017; Claar et al., 2023). Based on the EEG/EMG monitoring results, the combined administration of DMED and ESZ significantly reduced the duration of wakefulness (Figure 3A), prolonged the duration of NREM sleep (Figure 3B), and this effect was markedly superior to that of individual drug administration. This aligns with previous studies indicating that hypnotic drugs typically alter total sleep time and NREM sleep rather than REM sleep (Bajwa and Kulshrestha, 2013; Hajiaghaee et al., 2016; Yoon and Cho, 2018; Kim et al., 2019; Shi et al., 2019). From a functional perspective, NREM sleep plays a critical role in bodily recovery, energy conservation, and memory consolidation (Sun et al., 2020). The extension of NREM sleep by the combined treatment suggests its significant potential in promoting physiological maintenance and enhancement. Adequate NREM sleep facilitates protein synthesis and the repair of damaged tissues, which are essential for growth,



development, and daily recovery (Tononi and Cirelli, 2014). This indicates that the combined treatment may improve overall sleep quality by enhancing the physiological functions associated with NREM sleep. Furthermore, the prolongation of NREM sleep may positively impact cognitive functions. DMED has been shown to protect neurocognition by reducing interleukin (IL)-6 and IL-1 $\beta$  in

the hippocampus (Wang et al., 2019; Mei et al., 2021). It also improves cognitive function by reducing inflammation via  $\alpha_2$ -AR- mediated decreases in IL-1 $\beta$  and NF- $\kappa$ B levels (Li et al., 2020). ESZ can effectively improve the sleep quality in patients with sleep disorders,

reduce the number of nocturnal awakenings, and thereby enhance cognitive function (Huo et al., 2022). The significant increase in NREM sleep in this study suggests that the combined treatment may improve cognitive ability in mice. This finding provides a new theoretical basis for the clinical application of combined drug therapy. In the sleep cycle, NREM and REM sleep alternate, and the balance between the two is crucial for maintaining normal sleep and physiological functions. Although the combined treatment in this study did not significantly affect REM sleep (Figure 3C), the extension of NREM sleep may indirectly influence the functions related to REM sleep. Future studies could further explore the effects of combined treatment on the alternating patterns of NREM and REM sleep throughout the sleep cycle. The c-Fos protein, a product of the immediate-early gene c-fos, serves as a marker of neuronal activity and is widely used to study functional anatomy and neuronal activation states in the nervous system (Zant et al., 2016). As studies have indicated, the VLPO and TMN play central and well-defined roles in regulating the sleep-wake cycle (Chung et al., 2017; Scammell et al., 2019). By focusing on the VLPO and TMN, we can target the core components of the sleep-wake regulatory network. In this study, using c-Fos immunofluorescence staining, we investigated

the effects of combined DMED and ESZ administration on neuronal activity in the VLPO and TMN brain regions. VLPO

neurons primarily release inhibitory neurotransmitters, GABA and glycine. Existing studies have comprehensively demonstrated the central role of the VLPO in sleep initiation and maintenance through various perspectives, including neurotransmitter regulation (Gaus et al., 2002), environmental influences (Gong et al., 2000), and circuit mechanisms (Cirelli and Tononi, 2000), as evidenced by c-Fos immunohistochemistry. In contrast to the VLPO, the TMN is a key nucleus for maintaining wakefulness and is the sole source of histaminergic (His) neurons (Yu et al., 2014). In 2005, Saper and colleagues proposed the “flip-flop switch model” for sleep-wake transitions, which hypothesizes that sleep- promoting neurons in the VLPO and wake-promoting neurons in the TMN mutually inhibit each other to facilitate sleep-wake transitions (Saper et al., 2005). Our results showed that the combined treatment increased the number of c-Fos positive neurons in the VLPO (Figures 4C,E) while decreasing the number of c-Fos positive neurons in the TMN (Figures 4D,F). These findings align with the “flip-flop switch model,” further supporting the hypothesis that the combined administration of DMED and ESZ promotes sleep by modulating neuronal activity in these two brain regions. Additionally, the effect of sleep-inducing drugs on the VLPO is closely associated with the prolongation of NREM sleep. During NREM sleep, VLPO neuronal activity increases, leading to elevated expression of c-Fos protein, the product of the c-fos gene. Studies using optogenetics have shown that inhibiting the excitability of histaminergic neurons in the TMN during wakefulness can induce NREM sleep but not REM sleep (Venner et al., 2016; Yamashita and Yamanaka, 2017), which is consistent with our experimental results showing that the combined treatment suppresses REM sleep while enhancing NREM sleep.

The regulation of sleep and wakefulness is widely recognized to be related to the levels of corresponding neurotransmitters (Holst and Landolt, 2018). And NE, DA, Ach, Glu, and His as

excitatory neurotransmitters play a role in initiating and maintaining wakefulness in the sleep-wake cycle, and 5-HT, 5-HIAA, and GABA as inhibitory neurotransmitters can induce and maintain sleep state. The results of the present study showed that the combination of DMED and ESZ significantly decreased the levels of DA, NE, Ach, Glu, and His, while increasing the levels of 5-HT, 5-HIAA, and GABA, suggesting that the combination synergistically promotes the molecular mechanism of sleep through the bi-directional regulation of

excitatory-inhibitory neurotransmitter balance. DMED, as an  $\alpha$ 2-AR agonist, negatively feeds back by inhibiting the activity of NEergic neurons in the LC and reduces NE release (Bajwa and Kulshrestha, 2013), while ESZ may indirectly reduce NE levels by enhancing GABAergic inhibition. NE levels were significantly reduced after the combination in this study (Figure 5A), suggesting that the two drugs may reduce arousal drive by synergistically inhibiting the LC-NE pathway. The dopaminergic neurons are mainly located in the VTA and substantia nigra compacta (SNc) of the midbrain, with extensive fiber connections to the sleep-wake brain regions, and their dopaminergic signals projected to the forebrain play a key role in maintaining arousal and motivational behaviors (Montero et al., 2021). DA levels were significantly reduced in the present study (Figure 5B), suggesting that the combination may reduce arousal drive by inhibiting dopaminergic neuronal activity in the VTA and SNc. Noradrenergic neurons project to the VTA via the medial forebrain bundle (MFB). During wakefulness, VTA dopaminergic neurons exhibit activation states, whereas inhibition of these neurons promotes sleep (Eban-Rothschild et al., 2016). DMED, through its suppression of noradrenergic signaling, attenuates excitatory drive to VTA-DA neurons, thereby reducing dopamine (DA) release. ESZ, a GABA-A receptor agonist, exerts its effects by potentiating GABAergic inhibitory signaling. DA neurons in the VTA and SNc receive GABAergic projections from the ventral pallidum and nucleus accumbens, which directly suppress DA neuronal activity. Concurrently, enhanced GABAergic tone inhibits cortical and limbic dopaminergic systems, further reducing DA release (Tan et al., 2012). His is secreted only by histaminergic neurons in the TMN brain region, whose nerve fibers project widely throughout the brain and are essential for maintaining arousal (Scammell et al., 2019), and the reduction in His levels after the combination is consistent with the reduction in c-Fos positive neurons in the TMN (Figure 5C). This further supports the finding that inhibition of TMN activity is an important mechanism for sleep promotion. Acetylcholinergic neurons are mainly located in the LDT and PPT of the brainstem. Acetylcholine (ACh), which is involved in sleep regulation, is released from the terminals of these neurons and widely projects to the cerebral cortex, amygdala, hippocampus, thalamus, brainstem, and midbrain to promote arousal (Jones, 2020). Glu drives arousal in the thalamo-cortical loop (Dash et al., 2009). The significant decrease in Ach and Glu after the combination suggests that the two drugs may synergistically attenuate arousal signaling through inhibition of thalamo-cortical glutamatergic transmission and basal forebrain acetylcholinergic activity (Figures 5D,E). GABA, as a major inhibitory neurotransmitter in the central nervous system (CNS), mediates sleep via GABA-A receptors in areas such as the VLPO and basal forebrain (Scammell et al., 2017; Cai et al., 2023), ESZ acts as a GABA-A receptor agonist and directly enhances

GABAergic inhibition, whereas DMED may have a synergistic effect by inhibiting noradrenergic release and deregulating inhibition of GABAergic neurons. The GABA content in this study was

significantly elevated after the combination (Figure 5F), suggesting that the two drugs amplify GABAergic signaling through a dual mechanism (direct activation of receptors and deregulation of upstream inhibition). 5-HT neurons in the DRN exhibit complex modulatory roles in sleep-wake transitions, with their primary metabolite being 5-HIAA (Oikonomou et al., 2019). Accumulation of 5-HT may promote sleep through activation of 5-HT2A receptors. The elevation of 5-HT and 5-HIAA in the present study may reflect the modulation of the DRN-5-HT system by the combination of drugs (Figures 5G,H), but the exact mechanism needs to be further investigated. The initiation of REM sleep is associated with suppression of 5-HT and NE neurons, potentially mediated by activation of the lateral habenula (LHb) (Zhao et al., 2015; Takahashi et al., 2022). In this study, the sustained inhibition of NE may establish permissive neurochemical conditions for REM sleep. Notably, 5-HT has been demonstrated to activate the claustrum while inhibiting theta rhythm-promoting brain regions (Hajos et al., 2003; Nuñez and Buño, 2021). This dual action aligns with the insignificant REM sleep changes observed in the current study, potentially explaining why REM sleep remained unaffected.

## 5 Conclusion

For the first time, this research shows that DMED and ESZ work together to regulate sleep in mice. It also explains how this impact could work by looking at changes in neurotransmitter content, c-Fos protein expression, and sleep phases. This discovery paves the way for the creation of new medications that regulate sleep and offers strong theoretical support for the use of combination therapy in the treatment of sleep problems in clinical settings.

## References

In 2013, Bajwa and Kulshrestha published a paper. An adjuvant with significant clinical advancements is dexmedetomidine. Doi:10.4103/2141-9248.122044 Ann. Med. Health Sci. Res. 3(4), 475-483.

The authors of the article are Bao, Xu, Pan, Wang, Han, and Qu (2021). Sevoflurane anesthesia modulates states of consciousness via nucleus accumbens neurons expressing dopamine D1 receptors. Current Biology, Volume 31, Issue 9, Pages 1893–1902 (e5), doi:10.1016/j.cub.2021.02.011.

In 2023, Baranwal, Yu, and Siegel published a paper. The science of sleep, its disorders, and how to improve your sleep hygiene routine. The article is titled "Prog. Cardiovasc Dis. 77, 59-69" and the DOI is 10.1016/j.pcad.2023.02.005.

The authors of the manuscript are Cai, P., Zhang, J. S., Liu, P. C., Liu, F., Liu, R. F., and others (2023). Basal forebrain GABAergic neurons mediate behavioral and cerebral recovery from isoflurane anesthesia. The citation for this article is "J. Neurosci. 43 (16), 2907-2920" with the DOI=10.1523/jneurosci.0628-22.2023.

In 2022, Chima, Mahmoud, and Narayanasamy published a paper. How does dexmedetomidine fit into the world of contemporary critical care and anesthesia? Advanced Anaesthesia, Volume 40, Issue 1, Pages 111–130, DOI: 10.1016/j.aan.2022.06.003.

The authors of the article are Chung et al. (2017) and Weber et al. Using retrograde labeling and gene profiling, preoptic sleep neurons have been identified. The citation for this article is Nature 545 (7655), 477-481, with the DOI reading 10.1038/nature22350. In 2000, Cirelli and Tononi published a work. Regarding the importance of c-fos induction in the sleep-waking cycle from a functional standpoint. Doze off doi:10.1093/sleep/23.4.9, pages 9–25, volume 23, issue 4.

The Ciucă Published in 2023 by Anghel, D. M., Nițescu, G. V., Tiron, A. T., Gutu, C. M., and Baconi, D. L. Comprehending the impacts and processes of drug misuse. The article may be found in Molecules, volume 28, issue 13, and has the DOI number of Molecules28134969.

Citation: Claar et al. (2023) cites Rembado, Kuyat, Russo, Marks, and Olsen. Interactions between the corticothalamus and the brain influence the electrically induced EEG responses in mice. Publication date: 12 April 2019; DOI: 10.7554/eLife.84630.

In 2018, Crowe and Stranks published a paper. An updated meta-analysis of the cognitive effects of benzodiazepines: their residual effects in the medium and long term. The published version of this article is 33(7), 901-911 and may be accessed at doi:10.1093/arclin/acx120.

Tononi, G., Cirelli, C., Vyazovskiy, V. V., Douglas, C. L., and Dash, M. B. (2009). Stability of extracellular glutamate in the rat brain throughout sleep and wakefulness over the long term. *Journal of Neuroscience*, 2009, 29, 3, 620-629, doi:10.1523/jneurosci.5486-08.

A group of researchers including Dimitrios, Charmaine, Bengi, Roy, Robert, and Dara published a study in 2020. Both healthy and schizophrenic patients have sleep-dependent memory consolidation, but eszopiclone impairs this process. Publication date: 2020-02-450 *Biol. Psychiatry*, volume 87, pages 170-S171.

In 2022, the authors were Dong, H., Chen, Z. K., Guo, H., Yuan, X. S., Liu, C. W., Qu, W. M., and several others.

Mice that have dopamine D(1) receptor-expressing striatal neurons are more likely to stay awake.

The current biology article is published in volume 32, issue 3, pages 600-613, with the DOI 10.1016/j.cub.2021.12.026.

An article published in 2024 by Duan, Peng, Qin, Li, Xu, Wang, and others is cited as Duan, W. Y., et al.

Esketamine activates the glutamatergic neurons in the paraventricular thalamus, which speeds up the awakening from isoflurane general anesthesia in mice. This article was published in the *British Journal of Anaesthesia* on page 334-342. The DOI is 10.1016/j.bja.2023.10.038.

In 2016, Eban-Rothschild, A., Rothschild, G., Giardino, W. J., Jones, J. R., and de Lecea, L. published their work. Insightful sleep-wake patterns are controlled by dopaminergic neurons in the ventral tegmental area (VTA). *National Journal of Neuroscience*, 19, 10, 1356-1366, doi:10.1038/nrn.4377.

The authors of this work are Fan et al. (2023) and Cheng et al. (2023). Dextromethorphan, a sedative/anaesthetic and  $\alpha$ (2) adrenoceptor agonist, stimulates many kinds of neurons in the ventrolateral preoptic region of male mice. The current working paper is ASN Neuro 15, and the DOI is 10.1177/17590914231191016.

In 2018, Feng, Dong, Qu, and Zhang published a paper. Mice with impaired sleep-wake regulation systems are more likely to experience the onset and maintenance of non-rapid eye movement sleep when given dexmedetomidine orally. Published in *Front. Pharmacol.*, volume 9, issue 1, and with the DOI 10.3389/fphar.2018.01196.

Journal Article: Foucquier and Guedj (2015). Analysis of medication combinations: present methodological landscape. You may get the article at this link: *Pharmacol. Res. Perspect.* 3 (3), e00149. doi:10.1002/prp2.149.

In 2002, Gaus, Strecker, Tate, Parker, and Saper published a paper. In several mammalian species, galaninergic neurons that are active during sleep are located in the ventrolateral preoptic nucleus. *Brain Research* 115 (1), 285-294 (in print). This sentence cannot be paraphrased as it is a DOI (Web of Science DOI) and not written in English.

Publication: 2017 by Gerashchenko, D., Pasumarthi, R. K., and Kilduff, T. S. Expression of genes associated with plasticity during sleep induction by eszopiclone." The article is published in *Sleep* and can be accessed online at doi:10.1093/sleep/zsx098.

In 2000, Gong, H., Szymusiak, R., King, J., Steininger, T., and McGinty, D. published research. Regulation of c-Fos protein expression in the preoptic hypothalamus in relation to sleep: impact of environmental temperature change. Citation: *Am. J. Physiol. Regul. Integr. Comp. Physiol.* 279 (6), R2079-R2088. doi:10.1152/ajpregu.2000.279.6.R2079.

Members of the research team include Hajiaghaee, R., Faizi, M., Shahmohammadi, Z., Abdollahnejad, F., Naghdibadi, H., Najafi, F. (2016). A behavioral and electroencephalogram (EEG) investigation of rats and mice showed that a hydroalcoholic extract

of Myrtus communis might change anxiety and sleep characteristics. *Drug and Pharmaceutical Biology*, Volume 54, Issue 10, Pages 2141-2148, DOI: 10.3109/13880209.2016.1148175. With contributions from M. Hajos, W. E. Hoffmann, and R. J. Weaver (2003). How 5-hydroxytryptamine(2C) receptors control activity in the septo-hippocampus. Citation: *J. Pharmacol. Exp. Ther.* 306 (2), 605-615. doi:10.1124/jpet.103.051169.

Czajkowski, S., Morlock, E. V., Satyshur, K. A., and Hanson, S. M. (2008). The gamma-aminobutyric acid type-A (GABA $\alpha$ ) receptor is structurally distinct from zolpidem and eszopiclone. In the *Journal of Medical Chemistry*, volume 51, issue 22, pages 7243-7252, with the DOI of 10.1021/jm800889m.

In 2019, He, Q., Chen, X., Wu, T., Li, L., and Fei, X. published a paper. A meta-analysis of observational research reveals that long-term users of benzodiazepines are at increased risk of developing dementia. "Journal of Clinical Neurology" (2019, 15(1), 9-19), doi:10.3988/jcn.2019.15.1.9.

In 2018, Holst and Landolt published a paper. Brain chemistry during sleep and wakefulness. *Sleep Medicine Clinical Journal*, Volume 13, Issue 2, Pages 137-146, DOI: 10.1016/j.jscm.2018.03.002.

This sentence is a citation for a publication by Hughes et al. (2021). Depression and sleep quality in a population with rheumatoid arthritis: a cross-sectional study. *Clin. Rheumatol.*, 40(4), 1299-1305, doi:10.1007/s10067-020-05414-8.

An article published in 2022 by Huo, Cheng, Li, and Xu. Efficacy of eszopiclone in treating sleep disorders and Alzheimer's disease in older adults: a randomized controlled study. The article may be found in *Brain Behaviour*, volume 12, issue 2, and has the DOI10.1023/brb3.2488.

Jones, Benjamin E. (2020). Circuits involved in wakefulness and sleep. Publication: *Neuropsychopharmacology*, Volume 45, Issue 1, Pages 6-20. DOI: 10.1038/s41386-019-0444-2.

In 2019, Kim, Jo, Hong, Han, and Suh published a study. Mixing GABA with L-theanine promotes NREM sleep and reduces sleep latency. *Pharmaceutical Biology*, Volume 57, Issue 1, Pages 65-73, DOI: 10.1080/13880209.2018.1557698.

This sentence is a citation for a work by Li, Lai, Pan, Zhang, and Maze (2020). To counteract cognitive loss in mice produced by lipopolysaccharide, dexmedetomidine acts as an anti-inflammatory agent via  $\alpha$ 2 adrenoceptors. Published in the *Journal of Anesthesiology*, Volume 133, Issue 2, pages 393-407, with the DOI number 10.1097/ALN.0000000000000390.

In 2019, Liang, Huang, Xu, Wei, Xiao, and Wang published a paper. A meta-analysis and comprehensive review of randomized, placebo-controlled studies using eszopiclone vs other treatments for primary insomnia. *Journal of Sleep Medicine* 62, 6-13. doi:10.1016/j.sleep. Spring 2019; 03.16

In 2021, Mei, B., Li, J., and Zuo, Z. Through the central  $\alpha$ 2A adrenoceptor, dexmedetomidine reduces inflammation and encephalopathy caused by sepsis. "Brain Behav. Immun. 91, 296-314." (doi:10.1016/j.bbi). 0.008 in the year 2020

In a recent publication, Montero et al. (2021) brought up a number of important findings. In vivo firing pattern in ventral tegmental region and substantia nigra dopaminergic neurons in mice is predicted by dendritic architecture. Article number: 769342 in *Front. Neural Circuits*, published in 2021; DOI: 10.3389/fncir.2021.769342.

In 2003, Nelson, Lu, Guo, Saper, Franks, and Maze published a paper. The sedative effects of the alpha2-adrenoceptor agonist dexmedetomidine are produced via a mechanism that is already present in the body. "Anesthesiology" 98 (2), 428-436." doi:10.1097/00000542-200302000-00024.

In 2021, Nuñez and Buño published a paper. Neuronal and circuit processes leading to behavior and the theta rhythm in the hippocampus. The following is the DOI for the article: *Front. Cell Neurosci.* 15 (649262), 649262.

This sentence is a citation for a work by Oikonomou, Altermatt, Zhang, Coughlin, Montz, Grdinaru, and colleagues (2019). The serotonergic raphe induces slumber in rodents and zebrafish. *Neuron*, volume 103, issue 4, pages 687-691, doi:10.1016/j.neuron.2019.05.038.

A group of authors include L. R. Pinto, Jr., L. R. Bittencourt, E. C. Treptow, L. R. Braga, and S. Tufik (2016). Insomnia treatment: eszopiclone vs. zopiclone. (Sao Paulo, Brazil): Clin. (71 (1), 5-9), 2016 (doi:10.6061/clinics/2016(01)). 02

Wang, Y., Wu, Y., Yang, Z., Li, L., Zhu, X., and Qiu, G. (2020). Dexmedetomidine reduces the degree of sedation in mice by activating dopamine neurons in the ventral tegmental region. Published in the Journal of Anesthesiology, volume 133, issue 2, pages 377–392, with the DOI number 10.1097/ALN.0000000000003347.

This sentence was written by Ramaswamy, S. M., Struys, M., and Nagaraj, S. B. in the year 2021. validation on a wide scale using machine learning: profound sedation caused by dexmedetomidine

resembles non-rapid eye movement stage 3 sleep. Article cited as "Sleep" with the DOI 10.1093/sleep/zsaa167.

This was published in 2018 by Ren, S., Wang, Y., Yue, F., Cheng, X., Dang, R., Qiao, Q., and others. When it comes to being awake, the paraventricular thalamus plays a crucial role. Volume 362, Issue 6413, Pages 429–434 (doi:10.1126/science.aat2512). "Science"

Writing in 2009, Revel, Gottowik, Gatti, Wettstein, and Moreau were all involved. A survey of experimental methods that cause disruptions in sleep in rodent models of insomnia. The reference for this article is Neurosci. Biobehav Rev. 33(6), 874-899, with the online publication date of 2009-03-02.